# Tariff-based load shifting for domestic cascade heat pump with enhanced system energy efficiency and reduced wind power curtailment

Khoa Xuan Le[a,*], Ming Jun Huang[a], Christopher Wilson[a], Nikhilkumar N. Shah[a], Neil J. Hewitt[a]

[a]*Centre for Sustainable Technologies, University of Ulster, Co. Antrim BT37 0QB, United Kingdom*

**Abstract**

Cascade air-to-water heat pumps may have good potential for retrofitting UK domestic buildings because they can directly replace existing fossil-fuel boilers without the requirement of considerable modifications to heat distribution systems. A widespread uptake of these heat pumps, however, would pose challenges to the grid. Furthermore, wind power generation has increased in the UK to achieve the target of decreasing $CO_2$ emissions by 2050, but there are high levels of wind curtailment due to the mismatch between electricity supply and demand. In this paper, a load shifting study for cascade heat pumps coupled with thermal energy storage addressing these issues is presented. The main objective is to find the best tariff-based schedule load shifting for cascade heat pumps, which can help to avoid peak demand periods while obtaining enhanced system energy efficiency and reduced wind energy curtailment. How the retrofit performance of the cascade heat pumps with load shifting is further investigated. TRNSYS was used to simulate the system performance validated against experimental results. Northern Ireland (UK) was selected as the evaluated scenario. Simulation results showed that the tank temperature set point of 75 °C and the storage size of 1.2 $m^3$ could wholly shift the cascade heat pumps' operation to off-peak periods. The best times to start the cascade heat pumps to charge the storage were at 3 am and 2 pm for the morning and afternoon heating demands, respectively. Compared to oil boilers, the cascade heat pumps applied the best load shifting could obtain lower running costs (16 – 34 %) and carbon emissions (20 – 37 %).

*Keywords:*
Cascade air-to-water heat pump, thermal energy storage, tariff-based load shifting, TRNSYS simulation, enhanced system energy efficiency, reduced wind energy curtailment.

*Corresponding author: Tel. +44 (0) 28 903 66413
*Email addresses:* `le-k@ulster.ac.uk or k.le@ulster.ac.uk` (Khoa Xuan Le),

**Nomenclature**

| | |
|---|---|
| $\dot{m}$ | volumetric flow rate $[l/s]$ |
| $\rho$ | density of water $[kg/m^3]$ |
| $C_p$ | water specific heat capacity [kJ/kg.K] |
| $COP$ | coefficient of performance of heat pump [-] |
| $E$ | Energy [kWh] |
| $T$ | temperature [°C] |

**Subscripts**

| | |
|---|---|
| $e$ | electric use |
| $house$ | house |
| $in$ | inlet |
| $out$ | outlet |
| $q$ | heat |
| $w$ | water |

## 1. Introduction

The domestic sector in the UK accounted for 29 % of total final energy consumption [1] and 16 % of all carbon dioxide emissions [2]. Within this sector, space heating and hot water demands heavily relying on fossil-fueled boilers were responsible for about 40 % of the total $CO_2$ emissions [3]. Since the UK has a binding target of decreasing up to 80 % of $CO_2$ emissions by 2050 in comparison to the 1990 levels [4], these demands in residential buildings should be decarbonised by replacing conventional fossil-fuel boilers with low carbon alternatives, such as air-to-water heat pumps (AWHPs).

Many studies investigated the retrofit performance of AWHPs in the UK. For example, Kelly and Cockroft [5] estimated the running costs and carbon emissions of AWHPs when retrofitted into residential buildings in Scotland. Cabrol and Rowley [6] analysed how the system of AWHPs integrated with underfloor heating performed in UK domestic dwellings. Both the Energy Saving Trust (EST) and Department of Energy and Climate Change (DECC) [7] carried out two main in-situ trials to assess the performance of AWHPs and ground source heat pumps.

Most of the aforementioned work focused on single-stage AWHPs, but these heat pumps are an improbable retrofit technology in the UK. This is because the UK domestic housing

m.huang@ulster.ac.uk (Ming Jun Huang), c.wilson@ulster.ac.uk (Christopher Wilson), n.shah@ulster.ac.uk (Nikhilkumar N. Shah), nj.hewitt@ulster.ac.uk (Neil J. Hewitt)

stock has been well established with fossil-fuel boilers in line with high temperature heating distribution systems (e.g. traditional wet radiators, piping, DHW tanks, etc.). The existing wet radiators were designed to work efficiently with the flow temperature of 75 °C and the return temperature of 65 °C as suggested by BS-EN 442-2:2014 [8]. Providing this high outlet water temperature makes single-stage AWHPs reduce efficiency and cause high compressor ratios, as mentioned in [9]. Therefore, high installation costs are as a result of the significant adjustments to the heat distribution systems to improve the system efficiency if these heat pumps are retrofitted.

Cascade AWHPs (CAWHPs) can mitigate the issues of high compressor ratios and acquire better performance at low ambient temperatures, compared to single-stage AWHPs when running at high temperature water supply (over 60 °C) [10]. Therefore, they can directly replace existing boilers without the requirement of considerable modifications to the heat distribution systems, thereby reducing installation costs and disruptions. The study by Le et al. [11] also showed that cascade heat pumps could obtain running cost and carbon emissions savings in comparison with low efficiency oil boilers.

A rising proportion of electricity generation from renewable sources (e.g. solar, wind, etc.) in combination with the widespread uptake of heat pumps has been considered as a solution for reducing carbon footprint at the domestic level. Nevertheless, a significantly increasing number of heat pumps retrofitted into residential buildings may pose some challenges to the electricity grid. A potential burden of heavy load on the low voltage distribution network which is highly likely to cause voltage dips and cable overloading is one of the problems needing to be considered [13]. Furthermore, renewable energy generation (especially wind energy) has increased in the UK, but there are high figures of wind curtailment because of the mismatch between electricity supply and demand [14]. Load shifting has been used as a means for mitigating the burden on the national utility and advancing proportions of wind energy integrated into the grid when an increasing number of heat pumps, cascade air-to-water heat pumps in particular, are retrofitted.

### *1.1. State of the art of cascade air-to-water heat pumps*

CAWHPs differs from single-stage AWHPs in the capability of providing high flow water temperature (over 65 °C) with better overall efficiency at low ambient temperatures. In terms of system design, the main difference between CAWHPs and single-stage AWHPs is that the former has two refrigerant cycles connected by an intermediate heat exchanger or a middle water loop, whilst the latter has only one refrigerant stage. According to the recent reviews of Chua et al [15] and Zhang et al [16], cascade heat pump systems were first invented by Ma et al [17] in 2001. These cascade heat pumps had a middle water loop to exchange the heat between two refrigerant cycles, as shown in Fig. 1a. Later on, many fellow researchers developed cascade heat pump systems further using intermediate shell-tube or plat-shell heat exchangers (Fig. 1b) instead of middle water loops. Nowadays, cascade heat pumps featured with intermediate heat exchangers are becoming popular.

In Fig. 1b, a CAWHP comprises two separate single-stage refrigeration cycles: the lower refrigeration cycle and the higher refrigeration cycle. The low cycle utilises the refrigerant R-410a, while the refrigerant R-143a is used in the high cycle. The refrigerant R-140a is capable of evaporating at low ambient temperatures and condensing at a comparatively low pressure and a temperature of approximately 45°C [18]. Then, the heat from the condenser of the low cycle is transferred to the evaporator of the high cycle via the intermediate heat exchanger, which causes the refrigerant R-134a to evaporate. This refrigerant is condensed at low pressures to transfer heat to the water side, which can bring the outlet water temperatures up to 80°C. Based on this state-of-the-art of the technology, CAWHPs can address the problems of high compressor ratios and high discharge temperatures occurring in single-stage AWHPs when attempting to lift the outlet water temperatures to high levels.

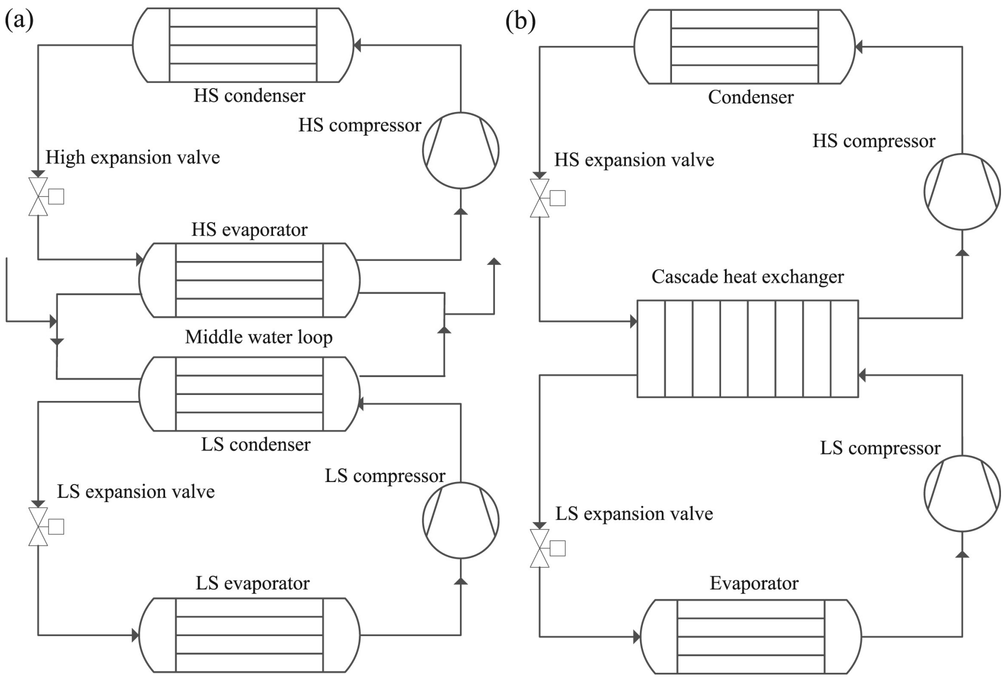


Figure 1: Schematic of a cascade heat pump featured with: (a) a middle water loop, (b) an intermediate heat exchanger [16].

### *1.2. Literature review on load shifting*

Thermal energy storage (TES) supporting heat pumps as a demand-side management (DSM) tool has played a significant role in avoiding the overload problems of the grid [19].

This coupling system can be used as a means for shifting load from peak-demand to low-demand periods. Such this system can also enable more proportions of renewable energy sources to be integrated into the grid. For example, the high figures of wind curtailment occurring at night (off-peak period) can be prevented if the thermal demands are shifted to this period thanks to the flexibility of TES coupled with heat pumps.

Load shifting from peak to off-peak hours of the system of heat pumps coupled with TES has become an attractive research topic. According to the extensive literature reviews of Fischer and Madani [20] and Pean et al.[21], there are two main control approaches to shift electrical heating or cooling demands: non-predictive control and model predictive control. While the latter has been found to outperform the former at achieving control goals (e.g. minimising running costs, maximising thermal comfort, etc.), the high costs of needing expertise in design and computational resources of a predictive model are such problems to be considered [20]. In contrast, non-predictive control can be simply designed without requiring many computational resources, but it still shows good performance and robustness.

Non predictive control can be categorised as: rule-based control and fixed scheduling. Rule-based control can be simply defined as if-then algorithms. Fixed scheduling is a DSM control approach in which the operation of heat pumps is blocked to the predefined hours to avoid peak power demand or high electricity rates. The predefined hours can be identified based on the already available information of a national electricity grid or the availability of static time-of-use tariffs. Fixed scheduling is simple and implemented easily, and it can obtain a substantial performance with better results than more advanced rule-based controls at some points [20]. Therefore, fixed scheduling is selected as a means of a DSM strategy for load shifting in this study.

There is much research about load shifting of heat pumps coupled with TES using predefined schedules. Kelly et al. [12] used a detailed simulation model in ESP-r software to carry out a system of an AWHP integrated with a buffering TES tank. The times to move the heat pump to off-peak periods followed a UK available time-of-use tariff. They found that 1 $m^3$ of hot water buffering or 0.5 $m^3$ of phase change material-enhanced hot water buffering was enough to shift the heat pump's operation fully to off-peak hours, without negatively influencing the provision of space heating and DHW for the final customers. Arteconi et al. [22] investigated a load shifting strategy for heat pumps coupled with buffering TES operating with radiators or underfloor heating distribution systems. The heat pumps were forced to switch off during peak hours defined by a time-of-use tariff in the UK to level off the grid power demand curve. However, these studies just focused on the system designs (e.g. optimal tank sizes, different system configurations) for the schedule load shifting strategies, whereas they did not truly conduct the optimal system operation efficiency to further obtain the control goals (e.g. minimised running costs, maximised thermal comfort). While the efficiency of an AWHP can be enhanced if it was shifted to hours where ambient temperatures were highest, this effect was not considered.

Whilst many studies investigated the enhancement of overall system efficiency of schedule load shifting heat pumps coupled with TES to acquire optimal control goals, most of them focused on one aspect of heating (either space heating or hot water heating). For example, Guo et al. [23] experimentally conducted an optimised operation strategy of a heat pump water heating system to minimise the operating costs. The optimal start-up time was between 12.00 h and 14.00 h where the ambient temperatures were high, and the electricity prices were low. Ibrahim et al. [24] examined the optimised system efficiency of a heat pump water heating system for Lebanon, with the operation of the heat pump was constrained to the low electricity rates and high ambient temperatures to minimise the running costs. Coninck et al. [25] conducted the system of a heat pump coupled with TES for space heating. The operation of the heat pump was moved to daytime to improve the overall efficiency to reduce energy consumption while still avoiding the high-demand hours of the grid.

There is the lack of information about how and when heat pumps and TES should operate interactively in shifting and meeting both space and hot water heating demands, with improved system operation efficiency to obtain better control goals. Furthermore, most of the cited publications on schedule load shifting focused on minimised running costs or reduced energy consumption rather than the aspects of renewable generation. Additionally, most of the aforementioned studies concerned single-stage AWHPs rather than CAWHPs providing high flow water temperatures. To the best of our knowledge, there is no study on CAWHPs coupled with TES applied schedule load shifting for both space and hot water heating at the domestic level to obtain both minimised running costs and reduced renewable energy curtailment.

### *1.3. Objectives of this study*

In this study, the schedule operation strategies for a CAWHP coupled with TES were designed to shift both space heating and hot water demand from peak to off-peak periods. The operation of the heat pump was blocked to off-peak periods identified by a time-of-use tariff. There are three main objectives of this study. The first is to find the best schedule to operate the cascade heat pumps efficiently with minimised running costs and reduced wind energy curtailment, while shifting wholly the electrical heating loads to off-peak periods.

The second is to find the optimum system design; storage tank sizing and temperature set points in particular. Finally, a retrofit assessment is carried out to evaluate how the designed load shifting strategy could help the cascade heat pumps save operating costs and carbon emissions when compared with the performance of gas and oil boilers.

## 2. Methodology

### *2.1. Structure of the simulations*

Fig. 2 shows the structure of the simulations carried out to obtain the results in this study. It contained two main parts: TRNSYS simulation tool and load shifting strategies. TRNSYS [26], a transient system simulation software, was used to model and simulate the studied system. The load shifting strategy component acquired the information inputs from the grid demand, the available electricity tariffs, the wind energy, the weather conditions, the tank sizes, the tank temperature set points, and the starting time to charge the storage tank. The TRNSYS simulation tool received the inputs from the load shifting strategy part, the developed and validated building models, and the weather conditions. Then, the TRNSYS tool provided the results of energy consumption, thermal output, running costs and system efficiency.

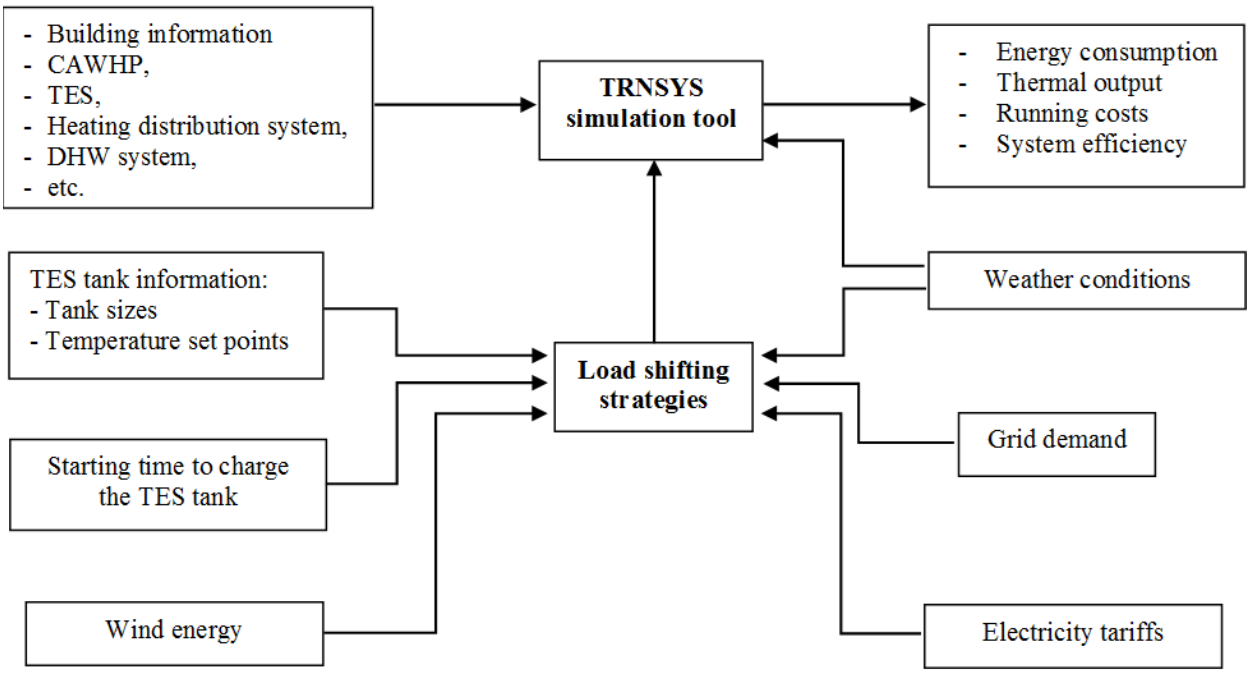


Figure 2: Structure of the simulations carried out in this study.

### 2.2. Building and heating system reference

The building investigated in this study was a mid-terraced hard-to-heat house representing typical ageing house stock in the UK. Fig. 3 shows two mid-terraced hard-to-heat buildings that were built at Jordanstown campus, University of Ulster, Northern Ireland (the UK), under the 1900s design specifications for research purposes. In this study, the house to the left in Fig. 3 was used as a case study. The building was inhabited by a family of three people, including two adults and one teenager.

Figure 3: Overview of two mid-terraced hard-to-heat buildings used for the study [27].

The building had two floors. The ground floor comprised living and kitchen areas, while the first floor was the spaces of three bedrooms and a bathroom. The external walls comprised of 215mm fair faced clay bricks and 15mm inner plaster insulation. The garret ceiling consisted of 19mm ply flooring and 150mm quilt insulation and 15mm plaster board, and the pitched roof was constructed of resin slate tiles lying on timber battens with the support of DuPont Tyvek vapor barriers. The floors comprised of timber covering by carpets, with the vented space below the flooring. Timber double-glazed windows and doors were assembled on the external walls. The summary of the building characteristics can be seen in Table 1.

Table 1: Summary of the case study building's characteristics.

| | Element | Value |
|---|---|---|
| Heated area ($m^2$) | Ground floor | 110 |
| | First floor | 150 |
| U-value ($W/m^2K$) | External wall | 1.65 |
| | Roof | 1.42 |
| | Floor | 0.67 |
| | Window | 4.8 |
| | Garret ceiling | 1.07 |
| | Door | 0.422 |
| Infiltration rate (ACH) | | 1.15 |

The heating system comprised a CAWHP coupled with a TES tank, transferring heat to the domestic hot water (DHW) and wet radiator systems for the space heating demand with the nominal flow of 75°C. Schematic of the heating system can be seen in Fig. 4. The CAWHP was a commercially available unit, and the TES was a custom-made product.

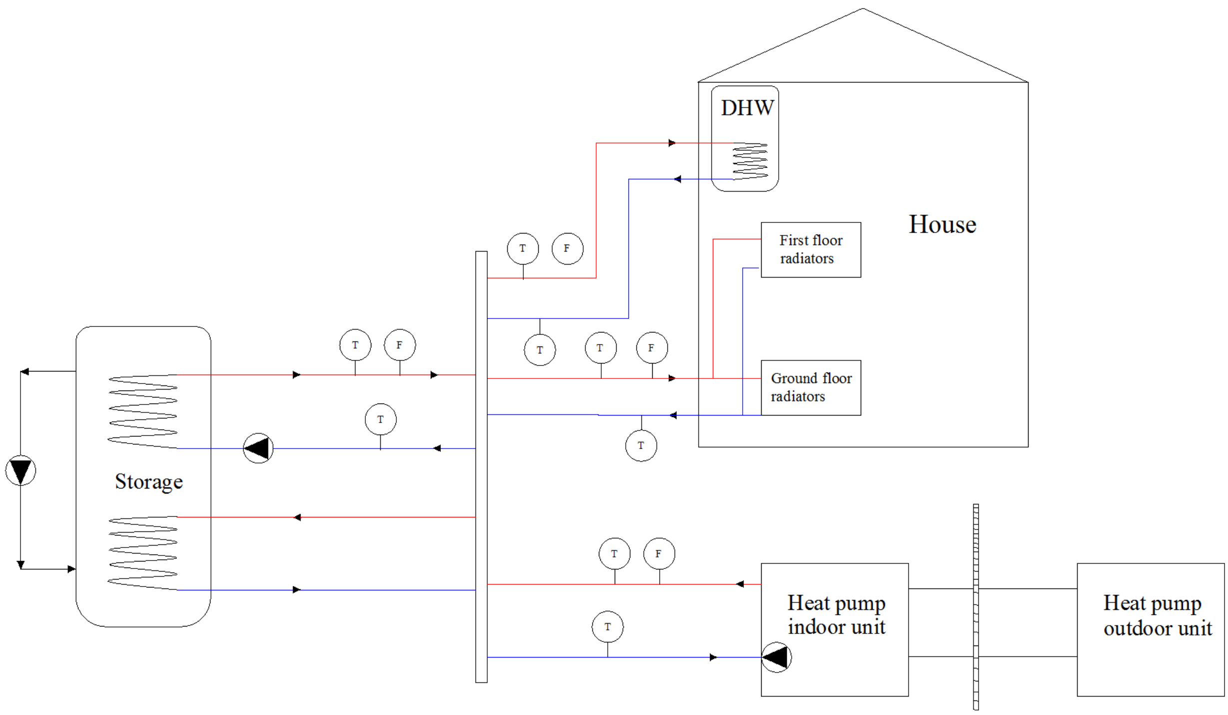


Figure 4: Schematic of the heating system of the building investigated in this study [11].

The indoor and outdoor units of the CAWHP employed R-134a and R-410A refrigerant, respectively. The nominal COP of the heat pump was 2.5 with the nominal heating capacity of 11 kW at 7 °C dry-bulb temperature of the heat source of the outdoor unit and 80 °C flow water temperature of the heat sink of the indoor unit, according to the manufacturer information [28]. The heat pump was an inverter unit, meaning that its heating capacity can be altered depending on the required thermal load.

The TES was a vertical cylinder using copper material with 75mm thick foam insulation. The investigated sizes of the TES in this study were in the range from 0.6 m$^3$ to 1.1 m$^3$. The tanks' height was 2 m, but their diameters were changed in accordance with the storage sizes. The charging heat exchanger coil was placed at the bottom part of the storage, while the discharging coil was located at the upper part.

The heating system was controlled on/off, based on a scheduled programmer to maintain the dining room temperature at 19.5 – 21 °C and the DHW temperature at 50 – 60 °C during the occupied hours. The periods of active occupancy and operation of the heating system are shown in Fig. 5, in which the data were adapted from the work of Kelly et al. [12] representing typical occupants' behaviors in the UK. In particular, the active occupancy was assumed to be 07.00 – 08.00 h and 18.00 – 23.00 h every day, and the heating system was turned on during the periods of 06.00 – 09.00 h and 16.00 – 11.00 h. The heating system was operated one hour earlier in the morning and evening than the occupancy periods to preheat the house.

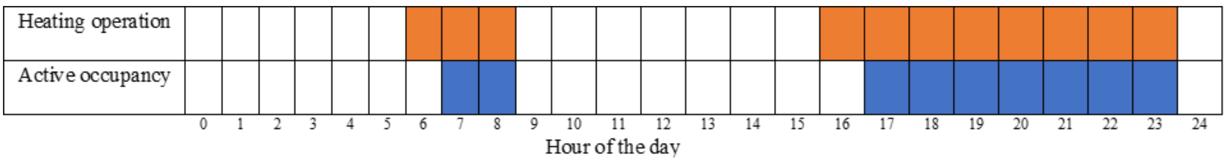


Figure 5: Daily operating hours of heating system and active occupancy (data are adapted from [12]).

### 2.3. TRNSYS modelling

TRNSYS [26] was used to model and simulate the studied system shown in Fig. 4. In this work, TRNSYS version 17 was obtained to develop the models as described clearly in our previous work [11]. The main components of the models are reported in Table 2. First, the building geometry was built in SketchUp software [29] and then imported into TRNSYS using Type 56. Then, the heating system was developed and implemented into the building model. Particularly, the CAWHP was modelled using Type 1217. This heat pump model mainly relied on a performance map containing full load and part load curves. Since this performance map did not include defrost cycles, an incorporating defrost model was developed outside the heat pump model. The TES tank was modelled using Type 534 which accounted for thermal stratification nature. The tank model had six fully mixed-equal volume segments, as the real tank mentioned above. Finally, the models of heat distribution system were developed and connected, comprising radiators (Type 1231), valves (Type 11 and Type 647), pipes (Type 31), temperature sensors (Type 911), pumps (Type 3d).

Table 2: Main components in TRNSYS environment used to simulate the studied system.

| Component | Description | TRNSYS Type | Source |
|---|---|---|---|
| Building | Building dimensions, envelops, thermal zones, internal heat gains, ventilations | Type 56 | Standard TRNSYS Type |
| CAWHP | Heat pump using performance map including full load and part load curves | Type 1217 | Non-standard TRNSYS Type (Commercial Library) |
| | Incorporating defrost operation | Type 2110 | Non-standard TRNSYS Type (Oliver et al. [30]) |
| TES | Thermal stratification tank consisting of six fully mixed-equal volume segments | Type 534 | Non-standard TRNSYS Type (TESS Library) |
| Radiators | Providing heat through a combination of radiation and convection without fans | Type 1231 | Non-standard TRNSYS Type (TESS Library) |
| DHW | Thermal stratification hot water tank | Type 534 | Non-standard TRNSYS Type (TESS Library) |
| Three-way valves | Distributing water flow | Type 11-f | Standard TRNSYS Type |
| | Mixing water flow | Type 11-d | Standard TRNSYS Type |
| Pipes | - | Type 31 | Standard TRNSYS Type |
| Pumps | - | Type 3d | Standard TRNSYS Type |
| Weather processing | Generating weather conditions based on data available in TRNSYS engine | Type 15-2 | Standard TRNSYS Type |
| Data reader | Generating historical data | Type 9a | Standard TRNSYS Type |
| Temperature sensors | Sensing room temperatures and water temperatures | Type 911 | Standard TRNSYS Type |

### 2.4. *Test and boundary conditions*

- **Grid demand**: In Fig. 6, the two-consecutive-day electrical demand in winter in all Ireland illustrates that the peak hours were from 16.00 h to 19.00 h, whereas the low demand was between midnight and 06.00 h. The control algorithms were designed to shift the house heating demands from peak hours to off-peak periods. Therefore, the TES tank played an important role. In particular, the TES supplied heat to the house during the period of 16.00 – 19.00 h, while it was charged to store the energy by the cascade heat pump at any time outside of that period. The start-up time to top up the TES was determined depending on the designed load shifting strategies, as explained in the next sections.

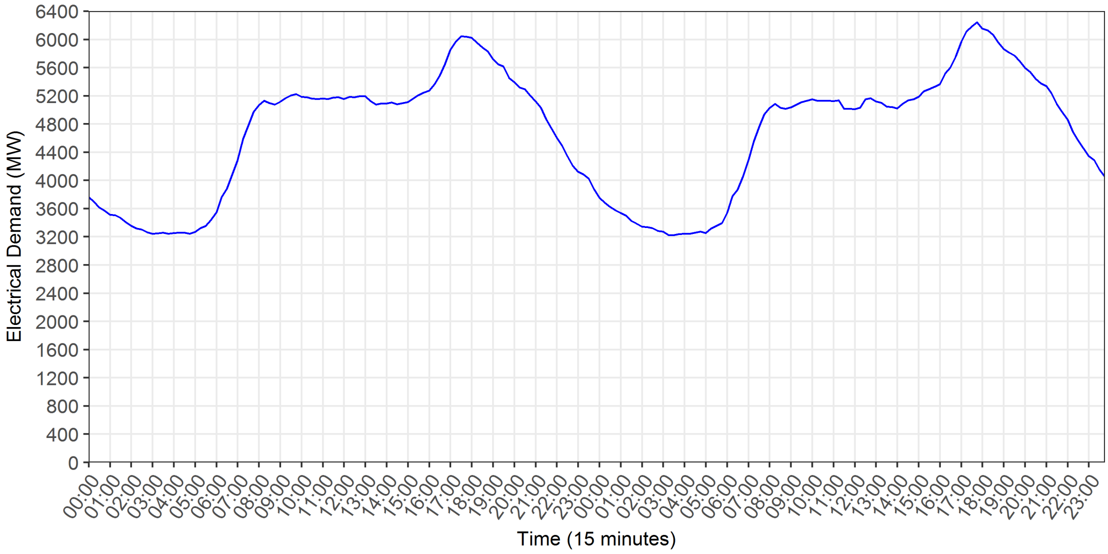


Figure 6: Two-consecutive-day grid demand in winter in whole Ireland (data are adapted from [31]).

- **Electricity tariffs**: In the UK, there are three main electricity tariffs, namely standard tariff, Economy 7 and Economy 10 in England (or Powershift tariff in Northern Ireland). In Northern Ireland particularly, the standard tariff is called a flat rate tariff in which the electricity rates are the same every day. The Economy 7 is a tariff in which the electricity price is much cheaper at night (01.00 – 08.00 h) compared to the flat rate, while the price in the daytime (09.00 – 24.00 h) is more expensive than the flat one. The Powershift can be defined as a time-of-use tariff, including three distinct rates: low rate applies between midnight and 08.00 h; normal rate is between 08.00 – 16.00 h and 19.00 – 24.00 h; peak rate applies from 16.00 – 19.00 h. In this study, the aims of the demand response control were to shift the heating demands from peak hours (16.00 -19.00 h) to off-peak periods. Therefore, the Powershift was an appropriate tariff for calculating the running costs of the cascade heat pumps in this study.

Furthermore, for comparison purposes, the flat rate tariff was applied to the reference case in which the heat pump was not controlled to shift the house heating demands, and the TES was not used. The electricity prices of the flat rate and the Powershift in Northern Ireland can be seen in Fig. 7.

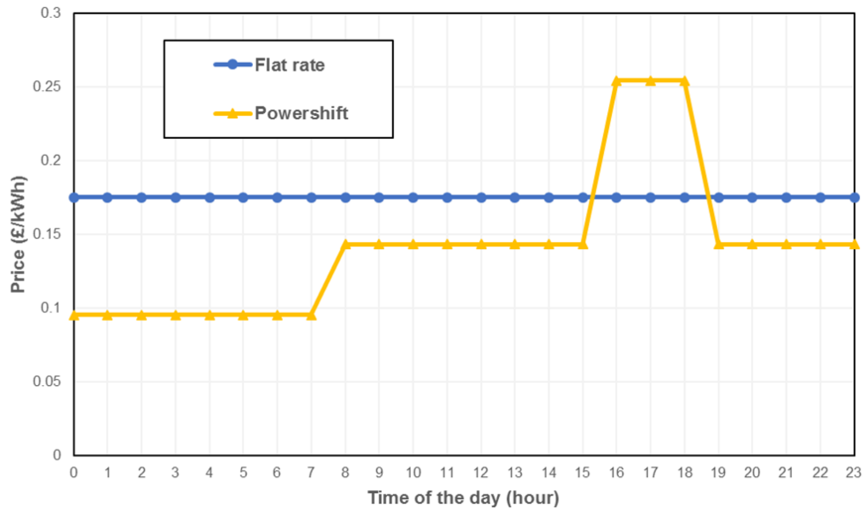


Figure 7: Electricity prices of the flat rate and the Powershift tariff in Northern Ireland [32].

- **Wind energy**: In Northern Ireland (the UK), there are high proportions of wind energy dispatch-down, according to the report of EIRGRID [14]. In Fig. 8, the highest figures are seen at night and in the afternoon. Therefore, the load shifting control strategies in this study were also designed to operate the cascade heat pump during the periods of the high wind curtailment power, which in turn can help more proportions of wind energy to be integrated into the grid.

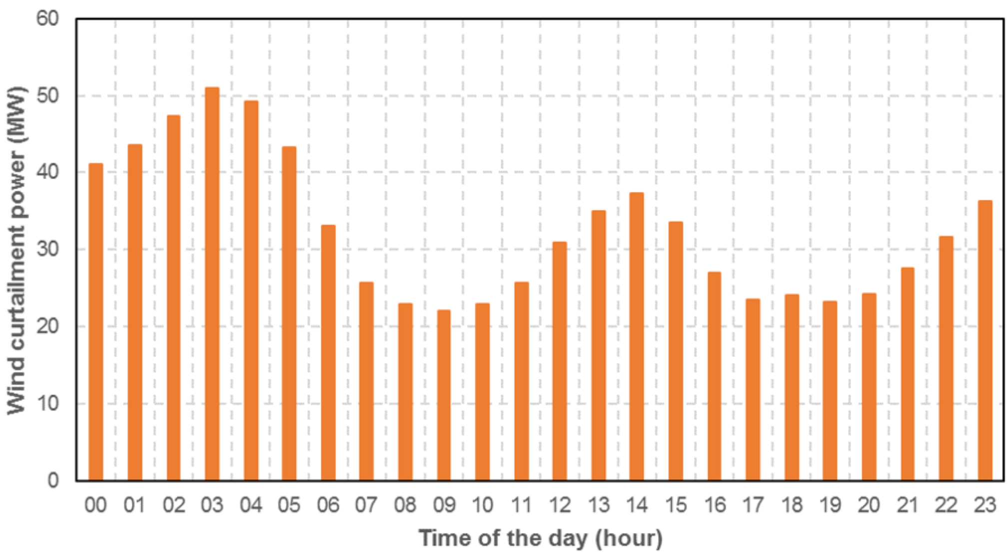


Figure 8: Northern Ireland average wind curtailment during the day in 2018 (data are adapted from [33]).

- **Weather data**: The weather data used to run the simulations were the Meteonorm data of Belfast - Northern Ireland (the UK), available in TRNSYS files. The average ambient temperatures versus 24 hours of winter, spring, summer and autumn are depicted in Fig. 9. The periods of each season in the UK can be defined as follows: winter is from December to February; spring is March – May; summer is between June and August; and autumn is September – November. It can be seen in the figure that, the trends of average temperatures of all seasons are similar. They are lower in the nighttime than in the daytime, and the highest air temperatures occur from 13.00 h to 16.00 h.

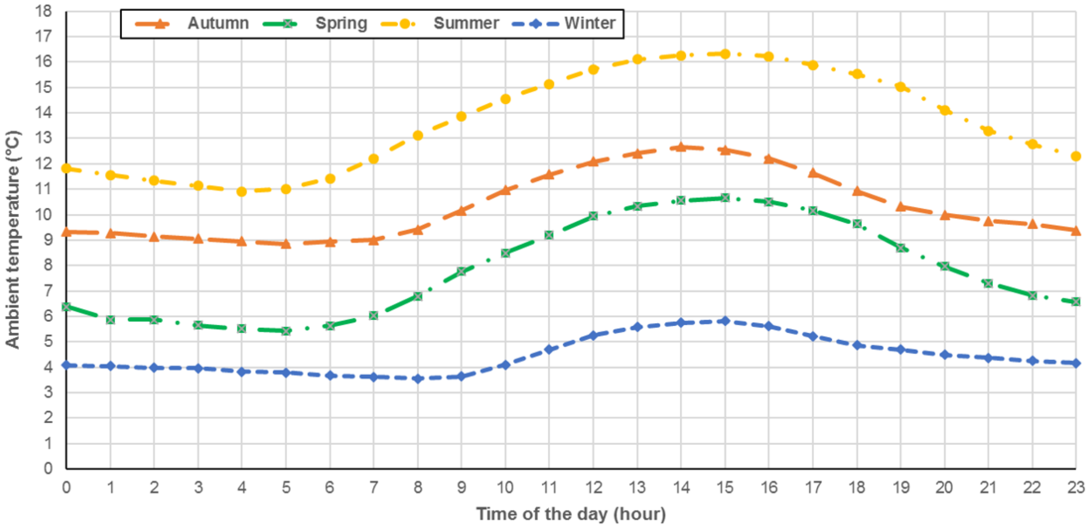


Figure 9: Average hourly ambient temperatures in each season in Belfast, Northern Ireland obtained from TRNSYS weather data.

- **The storage sizes and temperature set points**: Seven tank sizes were investigated in this study to evaluate the performance of the designed load shifting strategies. The sizes ranged from 0.6 $m^3$ to 1.2 $m^3$ with an increment of 0.1 $m^3$. Additionally, three different temperature set points of the tank were conducted, including 65 °C, 70 °C and 75 °C. There are two main reasons why the investigated tank set points were limited from 65 °C to 75 °C. First, if the tank set point is higher than 75 °C, the heat pump needs to lift its outlet water temperatures approximately over 80 °C (about 5 °C difference to the set point of the tank) to maintain the heat transfer rate between the heat pump and the storage via the heat exchanger, as stated in [12]. This hence makes the heat pump being overload and reduce its efficiency. Second, if the tank set point is reduced below 65 °C, it would result in the larger tanks to store enough energy to shift wholly the heating demand to off-peak hours. Since the real TES was custom made, its heat losses were higher than the units that are currently available in the UK market. Its average heat loss coefficient found in the experimentally validated model mentioned in section 3 was about 2.5 W/m$^2$K. Therefore, the average heat loss coefficient of the TES carried out in the simulations with the applied DSM strategies was improved to 0.6 W/m$^2$K [22].

- **Periods of the storage tanks to get fully charged**: To decide what time of a day the cascade heat pump should be turned on to charge the TES, a set of simulations was initially run to determine the periods the TES could reach its temperature set points from the cut-off temperature (55 °C). The times for the TES tanks to get fully charged are detailed in Table 3. The smaller tanks with the lower set points could get fully charged in shorter periods than the larger tanks with the higher set points. The times to fully top up the TES ranged from 54 minutes to 164 minutes.

Table 3: Time for the TES fully charged and the determined starting time to top up the TES for different tank sizes and temperature set points.

| Tank size ($m^3$) | Tank temperature set point (°C) | Time for the TES fully charged | Starting time to charge the TES (hour) | | |
|---|---|---|---|---|---|
| | | | Strategy A | Strategy B | Strategy C |
| 0.6 | 65 | 54 | 4 am | 2 pm | 4 am and 2 pm |
| | 70 | 68 | 4 am | 2 pm | 4 am and 2 pm |
| | 75 | 84 | 4 am | 2 pm | 4 am and 2 pm |
| 0.7 | 65 | 62 | 4 am | 2 pm | 4 am and 2 pm |
| | 70 | 79 | 4 am | 2 pm | 4 am and 2 pm |
| | 75 | 97 | 4 am | 2 pm | 4 am and 2 pm |
| 0.8 | 65 | 70 | 4 am | 2 pm | 4 am and 2 pm |
| | 70 | 89 | 4 am | 2 pm | 4 am and 2 pm |
| | 75 | 111 | 4 am | 2 pm | 4 am and 2 pm |
| 0.9 | 65 | 79 | 4 am | 2 pm | 4 am and 2 pm |
| | 70 | 100 | 4 am | 2 pm | 4 am and 2 pm |
| | 75 | 124 | 3 am | 1 pm | 3 am and 2 pm |
| 1 | 65 | 87 | 4 am | 2 pm | 4 am and 2 pm |
| | 70 | 112 | 4 am | 2 pm | 4 am and 2 pm |
| | 75 | 137 | 3 am | 1 pm | 3 am and 2 pm |
| 1.1 | 65 | 95 | 4 am | 2 pm | 4 am and 2 pm |
| | 70 | 120 | 4 am | 2 pm | 4 am and 2 pm |
| | 75 | 150 | 3 am | 1 pm | 3 am and 2 pm |
| 1.2 | 65 | 104 | 4 am | 2 pm | 4 am and 2 pm |
| | 70 | 132 | 3 am | 1 pm | 3 am and 2 pm |
| | 75 | 164 | 3 am | 1 pm | 3 am and 2 pm |

*2.5. Load shifting strategies*

This study aimed to seek the best schedule of operation and the system design of the CAWHP coupled with the TES to minimise the running costs, reduce the grid power demand during peak hours and increase the proportions of wind energy generation, while guaranteeing the thermal comfort of the end-users. Therefore, three load shifting strategies were designed based on the available electricity tariff (Powershift tariff); the outdoor ambient temperatures; the utility peak hours (16.00 – 19.00 h); and the periods of high wind curtailment. The following subsections describe in detail how these control strategies were designed.

### 2.5.1. Strategy A

In this strategy, the cascade heat pump was turned on to charge the TES at nighttime when the electricity rate was lowest according to the Powershift tariff (Fig. 7), and the stored energy was later used during peak hours to satisfy the house heat demands. Other than that period, the heat pump provided heat directly to the house when the space and DHW demands were required. By this strategy, the system could take advantage of the lowest electricity while reducing the utility power demand during peak hours.

To determine when the TES was charged at the night, there were four main factors to consider. First, in Fig. 9, the ambient temperatures did not change much during these hours, within 1 °C difference. Therefore, COPs of the heat pump were not much different during this period. Second, it took about one hour to three hours, depending on the tank sizes and temperature set points, to get it fully charged (Table 3). Meanwhile, it needed to be sure that the TES got fully charged before the first house heat demands were called at 06.00 h (Fig. 5). Third, as the TES was charged at night and then used in the afternoon, its efficiency due to standing heat losses should be minimised. Finally, the percentages of the wind power curtailment were highest from 03.00 h to 05.00 h (Fig. 8). If the cascade heat pumps were used during these hours, it could help more proportions of this renewable energy to be integrated into the grid. Based on these factors, the hours to start charging the TES were at 03.00 h and 04.00 h depending on the tank sizes and temperature set points, as mentioned in Table 3.

### 2.5.2. Strategy B

In this strategy, the CAWHP was on to top up the TES at daytime between 09.00 h and 16.00 h to take advantage of the high ambient temperatures (Fig. 9) while getting the normal rate electricity price (Fig. 7). Then, the stored energy was used during peak hours. This operation could help the cascade heat pump improve its efficiency and shift the peak grid demand.

There were four main factors to determine what time the TES was topped up. The first factor was due to the ambient temperatures. Looking at Fig. 9, the ambient temperatures in 09.00 – 16.00 h were highest from 13.00 h to 16.00 h, so the TES should be charged during these hours. The second was of wind energy curtailment. In Fig. 8, the highest wind dispatch-down power was from 13.00 h to 15.00 h. The third and fourth factors were the standby losses of the TES and the times for the tank to get fully charged. As a result, the time to start the CAWHP to charge the TES was at 13.00 h and 14.00 h depending on the tank sizes and temperature set points, as reported in Table 3.

### 2.5.3. Strategy C

In this strategy, the cascade heat pump was on to top up the TES at both the nighttime and the daytime to take advantage of both the low electricity rates and the high ambient temperatures. Particularly, the nighttime stored energy was used for the house heat demands in the morning (06.00 – 09.00 h). As the electricity price was still lowest from 06.00 h to 08.00 h (Fig. 7) in the period of the morning demands, the cascade heat pump provided heat directly to the house for two hours (06.00 - 08.00 h), while the stored energy at the nighttime was used for only one hour (08.00 – 09.00 h) to satisfy the house demands. Additionally, the daytime stored energy was used during peak hours.

Considering the same factors as the above Strategy A and Strategy B, the hours to start the CAWHP to top up the TES were at 04.00 h and 14.00 h for the lower tank sizes and set points, while at 03.00 h and 14.00 h for the larger tanks and higher temperature set points. These are detailed in Table 3.

## 3. Experimental validation of the thermal energy storage model

The coupling models of the building and the CAWHP have been successfully validated against laboratory and in-situ results, as mentioned in the previous study [11]. Therefore, only experimental validation of the TES model is presented in this paper.

The experimental set-up shown in Fig. 10 was utilized to measure the tank temperatures. The size of the measured TES tank was 0.6 $m^3$, with 2 m height and 0.6 m diameter. There were seven temperature sensors (PT 100 thermocouples with uncertainties of ±0.2 °C) placed at an equal distance (0.33 m) along the vertical for control and monitoring purposes. There was also a de-stratification pump installed on the storage to mix thermally fully inside the tank if needed. The readings were logged in one-minute intervals by means of a desktop computer-based data acquisition system.

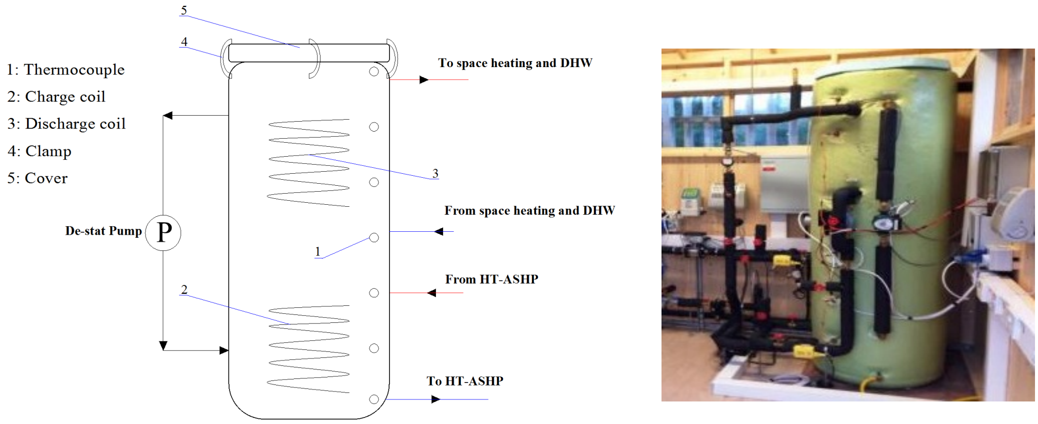


(a) Schematic of the measured TES tank.

(b) Experimental set-up of the measured TES in the laboratory.

Figure 10: Schematic of monitored storage tank and its experimental set-up [34].

The TES tank was connected to the CAWHP to supply heat to the house, as depicted in Fig. 4. First, the TES was charged from 55 °C to 75 °C by the heat pump at 01.00 h to store the energy. Then, there was a lag of about four hours between charging and discharging the stored energy to the house. Discharging ended when the store temperature dropped to 55 °C. After that, the tank was left for approximately 17 hours. During charging, discharging and the first standby periods, the stratification nature inside the storage was eliminated by turning on the de-stratification pump (as shown in Fig. 10), while the stratification effects occurred naturally in the second standby period. Based on this operation test, the experimental data could allow the TES model to be validated as of three modes: (1) charge, (2) discharge and (3) thermal standby losses, with and without stratification effects.

Fig. 11 illustrates the one-day comparison between the simulated and experimental results of the TES, with temperatures at the top and bottom segments being shown for clarity. Both the charging (01.00 - 02.10 h) and discharging (05.30 - 06.20 h) periods showed a good agreement between the simulation and the experiment. "Standby Loss 1" attained a good correlation. However, there were some discrepancies during "Standby Loss 2" (after 18.20 h), and stratification was noticed during this period. The simulated top node temperature in "Standby Loss 2" gradually overestimated the monitored top temperatures with the maximum of 2.5 °C, whereas the bottom temperatures seemed to coincide within the uncertainty of 1 °C.

The differences during "Standby Loss 2" were highly challenging to address, although the model parameters were fine-tuning. The tank nodes in TRNSYS were consistent, while the measured temperatures at different heights of the tank via thermocouples were not uniform. There were inlets/outlets of the heat exchangers and supply water along the tank which caused natural heat conduction with connected pipes as well as heat convection within the tank, and therefore the temperatures at the thermocouples close to those pipes decreased more suddenly than temperatures at the others. For example, the top tank node temperature of the monitored data in Fig. 11 decreased quickly after 16.00 h. Such the TES model, in contrast, did not consider this effect. Fortunately, these discrepancies were minor and acceptable.

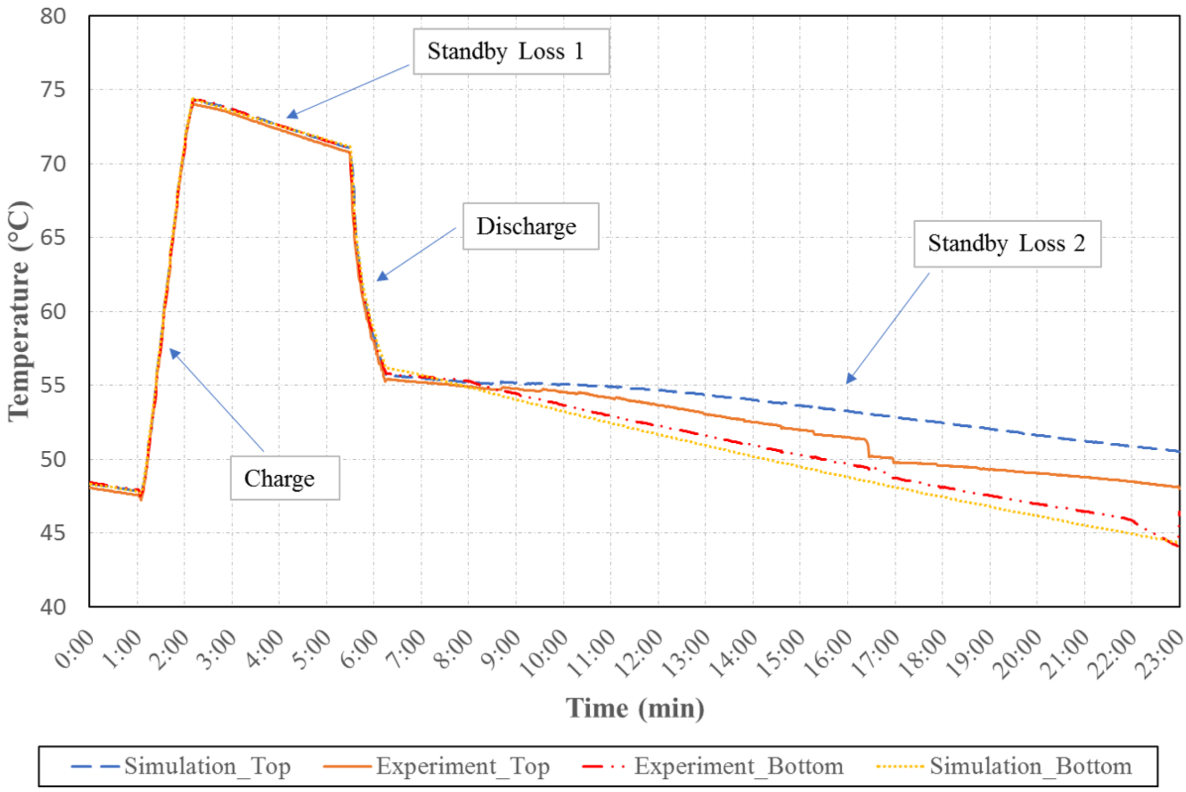


Figure 11: Simulated versus experimental results of the storage tank during charging, discharging and standby periods (the figure is adapted from our conference paper [34]).

## 4. Simulation results and discussion

### *4.1. Optimal tank sizes and temperature set points*

To find the optimal tank sizes and temperature set points for the designed load shifting control strategies, a set of simulations was carried out. 63 simulations in total were run interchangeably with different tank sizes and set points and three different control strategies. The simulations were run with one-minute steps for two winter months, January and February, where the ambient conditions were most severe in the year.

The summary of the simulation results is shown in Table 4. It includes the total running costs and the total energy consumption of the cascade heat pumps during peak hours. Looking at each control strategy in the table, if the tank sizes and temperature set points were lower, the running costs were higher. Similarly, the CAWHPs consumed more energy during peak hours if the tank sizes and temperature set points were lower. Therefore, the optimum tank size was 1.2 $m^3$, and the optimum temperature set points of the storage was 75 °C. With this system design, Strategy B and Strategy C could wholly shift three-hour peak demands.

Table 4: Total running costs and energy consumption during peak hours of the heat pump in two winter months applied the three load shifting strategies with different tank sizes and temperature set points.

| Tank temperature set point (°C) | Tank size ($m^3$) | Total running costs of the heat pump (£) | | | Total energy use of the heat pump during peak hours (kWh) | | |
|---|---|---|---|---|---|---|---|
| | | Strategy A | Strategy B | Strategy C | Strategy A | Strategy B | Strategy C |
| 65 | 0.6 | 401 | 406 | 392 | 657 | 615 | 631 |
| | 0.7 | 397 | 403 | 388 | 625 | 581 | 597 |
| | 0.8 | 392 | 400 | 383 | 592 | 546 | 563 |
| | 0.9 | 388 | 396 | 379 | 560 | 511 | 528 |
| | 1 | 383 | 393 | 374 | 526 | 476 | 493 |
| | 1.1 | 378 | 389 | 369 | 493 | 440 | 458 |
| | 1.2 | 373 | 386 | 364 | 459 | 404 | 422 |
| 70 | 0.6 | 388 | 396 | 379 | 564 | 517 | 530 |
| | 0.7 | 381 | 391 | 372 | 513 | 465 | 478 |
| | 0.8 | 373 | 385 | 365 | 463 | 412 | 425 |
| | 0.9 | 366 | 380 | 358 | 412 | 358 | 372 |
| | 1 | 358 | 375 | 351 | 400 | 305 | 320 |
| | 1.1 | 351 | 369 | 343 | 309 | 250 | 265 |
| | 1.2 | 344 | 364 | 336 | 256 | 196 | 216 |
| 75 | 0.6 | 374 | 386 | 367 | 469 | 417 | 427 |
| | 0.7 | 364 | 379 | 357 | 401 | 347 | 357 |
| | 0.8 | 355 | 371 | 347 | 334 | 276 | 285 |
| | 0.9 | 345 | 365 | 338 | 268 | 209 | 219 |
| | 1 | 335 | 357 | 328 | 197 | 135 | 148 |
| | 1.1 | 324 | 349 | 318 | 123 | 59 | 73 |
| | 1.2 | 314 | 344 | 309 | 49 | 0 | 0 |

### *4.2. Comparison of three load shifting strategies*

In order to compare the performance of the designed load shifting strategies, another set of simulations was run. The optimum tank size of 1.2 $m^3$ and the optimum tank temperature set point of 75 °C found in the previous section 4.1 were selected in these simulations. The simulations were run with one-minute intervals for a whole year period. Apart from the simulations for the three control strategies, one simulation, named Base Case, was run with the CAWHP providing heat directly to the house without the TES. This means that there was not load shifting in this Base Case.

Table 5 summaries the annual results of the investigated simulations. The useful heat output is defined in the following Eq. 1, which accounts for the heat losses of the whole system.

$$E_{q,house} = \int_0^t \rho \times C_p \times \dot{m}_{house} \times (T_{w,in,house} - T_{w,out,house}) \times \mathrm{d}t \tag{1}$$

Table 5: Summary of simulation results of three control strategies and Base Case.

| | Base Case | Strategy A | Strategy B | Strategy C |
|---|---|---|---|---|
| Annual useful heat output [kWh] | 21412 | 23442 | 23503 | 23619 |
| Annual energy consumption [kWh] | 9646 | 11911 | 11518 | 11869 |
| Annual wind curtailment prevention [kWh] | 8707 | 10687 | 10332 | 10697 |

As for energy consumption, the CAWHP in Base Case consumed least energy compared to the ones in the other control strategies, 9646 kWh per year (Table 5). The energy utilisation of the cascade heat pump was lower in Strategy B (11518 kWh/year) than in Strategy C (11869 kWh/year). The heat pump in Strategy A used the highest energy (11911 kWh/year).

With regards to running costs, although Strategy C made the cascade heat pump consume more energy than the ones in Base Case and Strategy B, its annual running cost was lowest (£1345), as shown in Fig. 12. Note that the flat rate tariff (£0.175/kWh) was applied to calculate the running cost of the heat pump in Base Case, while the Powershift tariff (low rate: £0.0953/kWh, normal rate: £0.143/kWh, peak rate: £0.254/kWh) was used for the cascade heat pump in three load shifting strategies. Strategy C was designed to take advantage of both the low electricity rates and the higher ambient temperatures, thereby improving its overall efficiency and reducing its running costs. Compared to Strategy B (£1545 per annum), Strategy A (£1368 per annum) obtained lower operating cost, meaning that the lower electricity rates played more important role than the higher ambient temperatures. Base Case was the worst system operation as its yearly operating cost was highest (£1688).

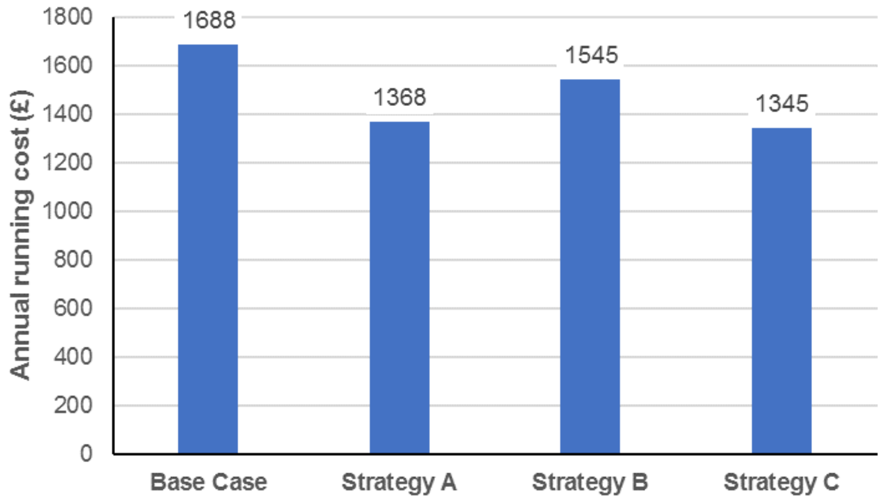


Figure 12: Annual operating costs of three control strategies and Base Case.

In terms of thermal comfort, Fig. 13 illustrates the total comfort time in the year of three load shifting strategies and Base Case. The total hours of comfort were calculated based on the time in which the room temperature was over the set point during the occupied periods. Considering three load shifting strategies, Strategy C could maintain better thermal comfort than the other two strategies. While Base Case was the most expensive operation as mentioned above, its thermal comfort was just slightly higher than the levels of Strategy B and Strategy C.


Figure 13: Total comfort hours in a year of three control strategies and Base Case.

To see how the designed control algorithms affected the utility demand power, the one-day impact figure of the CAWHPs applied the load shifting strategies along with the breakdown of energy consumption of the cascade heat pumps during off-peak and peak hours in the one-year period are illustrated in Fig. 14 and Fig. 15, respectively. Note that the cascade heat pump electrical demand in Fig. 14 was aggregated with 5% of the current housing stock in Northern Ireland (5% of 776526 buildings [35]), while the breakdown of energy utilisation in each figure in Fig. 15 accounted for only one single cascade heat pump. In Fig 14, it can be seen that the CAWHP without the load shifting would pose challenges to the grid as there was an added peak demand (maximum of about 300 MW) from 16.00 h to 19.00 h. Considering the cascade heat pumps with three load shifting, their operation was totally avoided during peak hours. In Fig 15, the annual energy use was separated into four periods representing the electricity rates in the Powershift tariff: low rate (0.00 – 08.00 h), normal rate (08.00 – 16.00 h and 19.00 – 24.00 h), peak rate (16.00 – 19.00 h). It can be seen in the figure that Strategy B and Strategy C could shift wholly the house demands from peak to off-peak hours for the whole year period, which in turn was beneficial for the utility power demand. Furthermore, according to Strategy C, the cascade heat pump consumed the highest level of energy during the night time (0.00 - 08.00 h) where the low grid demand was observed.

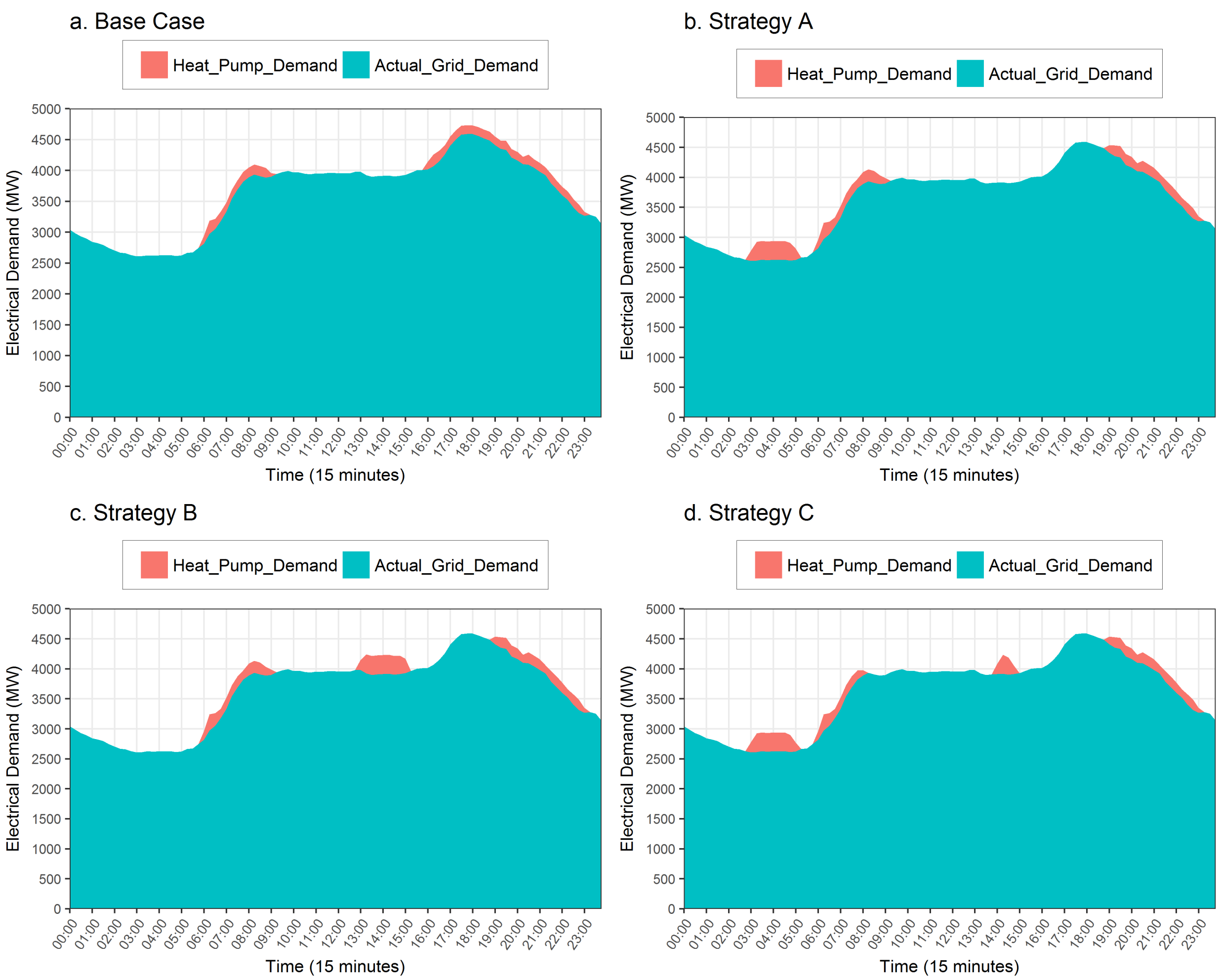


Figure 14: One-day impact of the cascade heat pump applied the load shifting strategies on the grid (the electrical power of the heat pump is aggregated with 5% of the current housing stock in Northern Ireland).

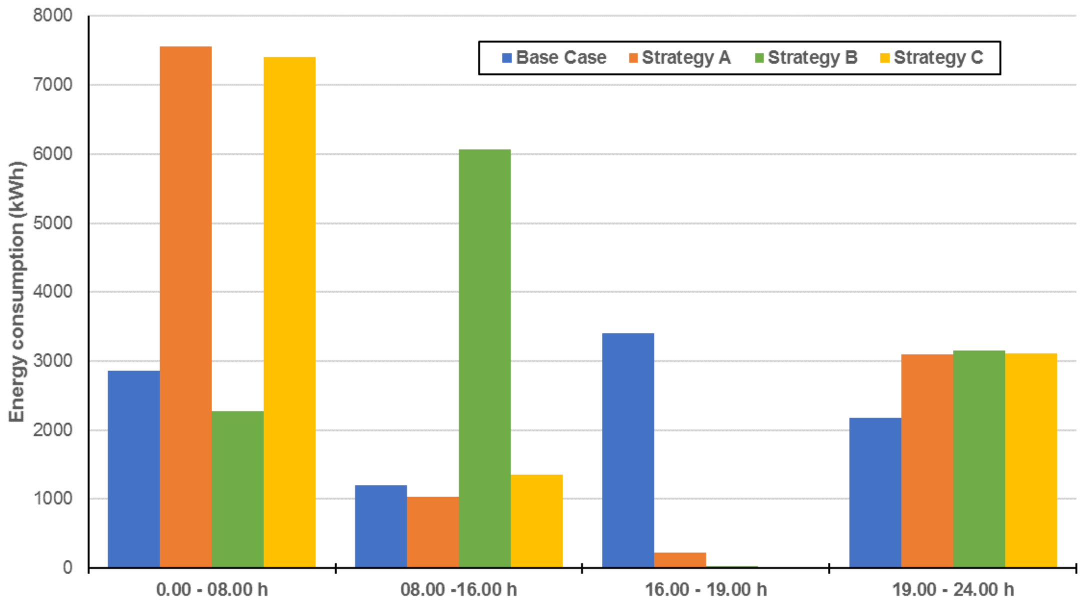


Figure 15: Breakdown of energy consumption of the heat pump in peak and off-peak hours.

How much wind energy curtailment could be prevented in Northern Ireland was also evaluated for the load shifting strategies. Fig. 16 shows an example of one-day wind curtailment power and the power consumption of the cascade heat pump to illustrate how the numbers of the wind curtailment prevention was calculated in Table 5. In particular, if the heat pumps operated during the periods of wind dispatch-down, it was assumed that wind energy would be used by the heat pumps. In Table 5, the amount of wind energy curtailment prevention was highest (10679 kWh) with the heat pump applied the load shifting Strategy C, while that was lowest (8707 kWh) with the heat pump operating without load shifting.

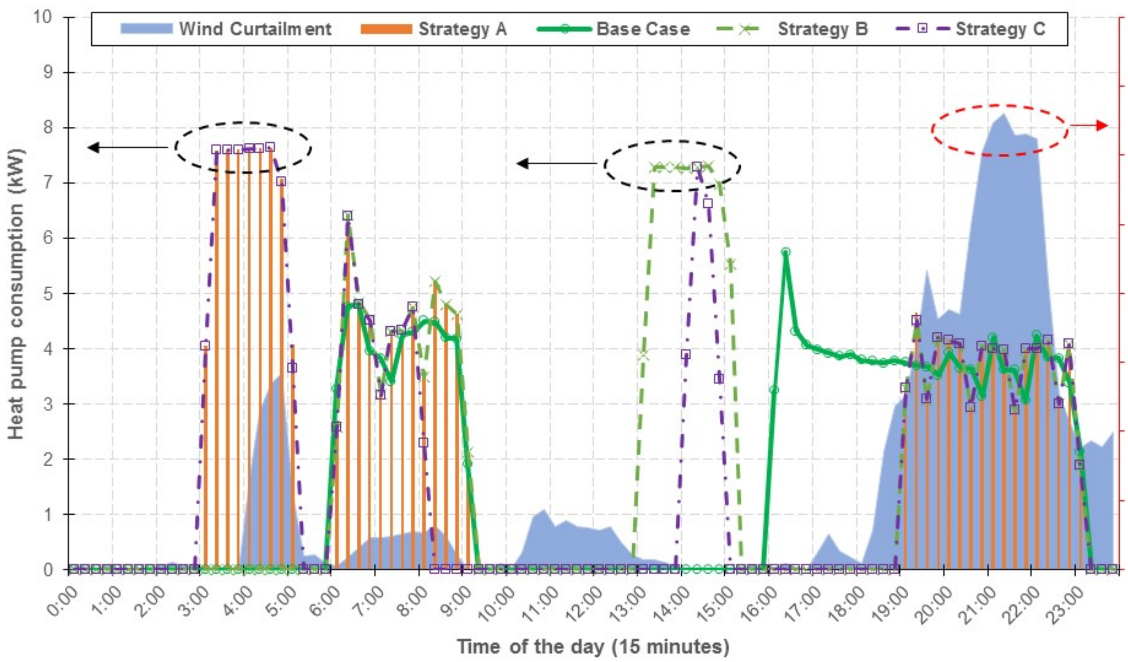


Figure 16: Example of one-day heat pump power consumption in three control strategies and Base Case along with wind curtailment power in Northern Ireland (wind dispatch-down data are of 2018 and adapted from [14]).

In short, it can be said that Strategy C was the best load shifting control strategy because it could help the CAWHP reduce annual running costs, maintain better levels of thermal comfort, perfectly avoid the grid power demand during peak hours and allow the highest proportions of wind energy to be integrated into the grid.

*4.3. Retrofit assessment of the cascade air-to-water heat pump applied Strategy C*

Since Strategy C yielded the best system operation compared to the other two strategies, as mentioned in the previous section, the performance of the CAWHP applied Strategy C was compared to the performance of gas and oil boilers to assess its retrofit ability in the UK. In particular, the running costs and carbon emissions of the 60, 70, 80 and 90 % efficiency gas and oil boilers were the measures to compare with the results of the cascade heat pump applied Strategy C. These boilers represent from old heavy weight boilers to new condensing boilers that are popular in the UK housing stock.

The summary of the comparison results can be seen in Table 6. The oil price was £0.068/kWh [36]. The gas price was £0.06508/kWh for the first 2000 kWh, and £0.0459 /kWh for the after 2000 kWh [37]. The carbon emissions factors were 0.2 kg$CO_2$/kWh and 0.243 kg$CO_2$/kWh for gas and oil, respectively [38]. Time-series carbon intensity on the grid of all Ireland in 2018 [33] was used to calculate the carbon emissions of the heat pump. One-week example of 15-minute carbon intensity data can be seen in Fig 17.

Table 6: Annual results of energy consumption, running costs and carbon emissions of the cascade heat pump applied Strategy C and boilers.

| | Efficiency (%) | Annual energy use (kWh) | Annual running cost (£) | Annual carbon emissions (kg) |
|---|---|---|---|---|
| Strategy C | - | 11869 | 1345 | 4562 |
| Oil boiler | 60 | 29977 | 2038 | 7284 |
| | 70 | 27836 | 1893 | 6764 |
| | 80 | 25694 | 1747 | 6244 |
| | 90 | 23553 | 1602 | 5723 |
| Gas boiler | 60 | 29977 | 1414 | 5995 |
| | 70 | 27836 | 1316 | 5567 |
| | 80 | 25694 | 1218 | 5139 |
| | 90 | 23553 | 1119 | 4711 |

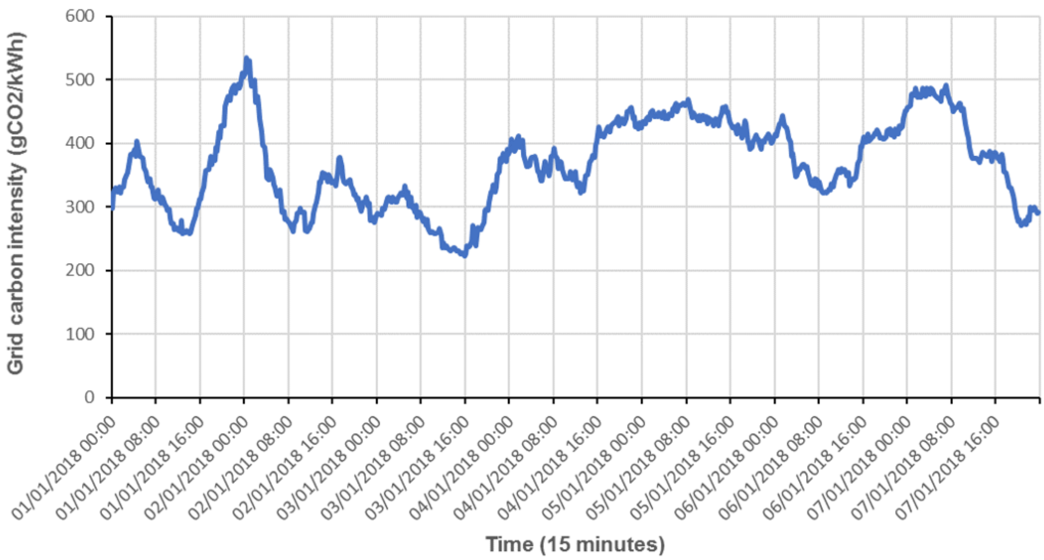


Figure 17: One-week carbon intensity on the grid of all Ireland in 2018 (data are adapted from [33]).

Fig. 18 illustrates the percentages of yearly operating cost savings of gas and oil boilers compared to the heat pump applied DSM Strategy C. The positive values in the figure indicate that the heat pump can obtain running cost savings compared to boilers, while negative values indicate the heat pump is more expensive to run than boilers. It can be seen in the figure that, if the CAWHP was retrofitted into the houses using oil boilers or low efficiency gas boiler (60 %), Strategy C could help the homeowners to save the running costs (from 5 % to 34 %). However, there were not cost savings if the houses used high efficiency gas boilers (over 70 % efficiency).

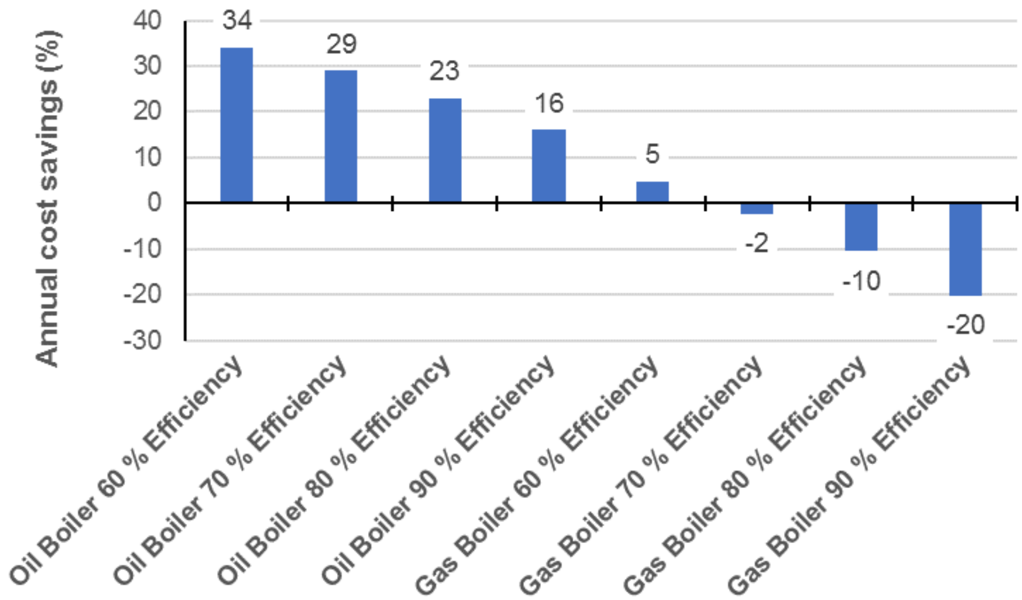


Figure 18: Annual running cost savings of the retrofit CAWHP applied Strategy C compared with boilers (positive values indicate the heat pump can obtain running cost savings compared to boilers, while negative values indicate the heat pump is more expensive to run than boilers).

In Fig. 19, the percentages of annual carbon savings of gas and oil boilers compared to the CAWHP with Strategy C. The positive values in the figure indicate that operating the heat pump emits less carbon than running boilers. It can be seen in the graph that there were carbon emission savings ranging from 3 % to 37 % if all oil and gas boilers were replaced by the heat pump applied Strategy C.

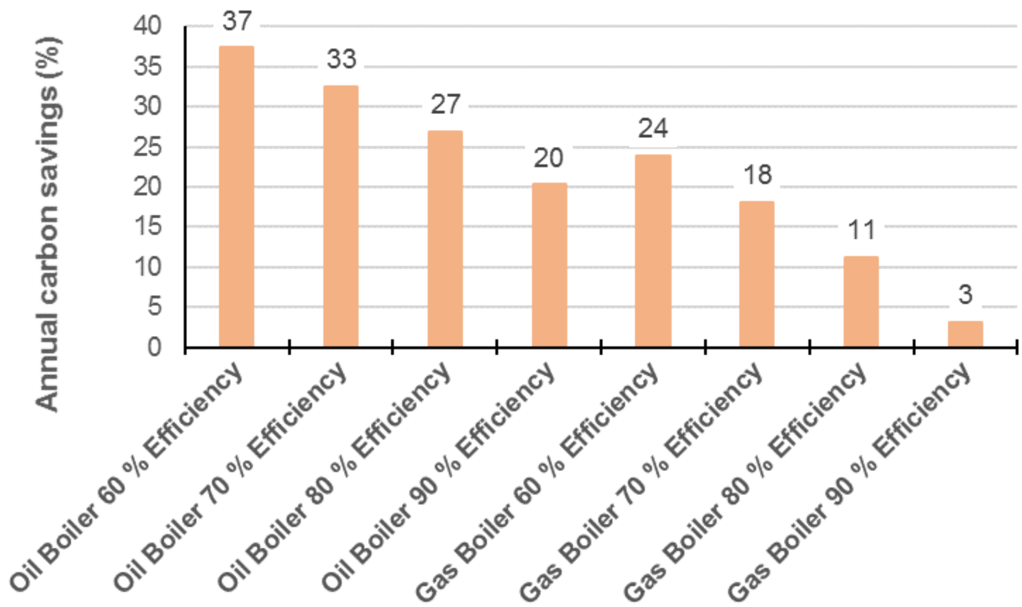


Figure 19: Annual carbon savings of the CAWHP applied Strategy C compared with boilers (positive values indicate that running the heat pump emits less CO2 than running boilers).

Although Strategy C could not help the cascade heat pump to acquire cost savings compared to the high efficiency gas boilers (over 70 %), there were cost benefits and carbon emissions savings if the CAWHP applied Strategy C was retrofitted into the houses using oil boilers. In the previous work [11], the CAWHP without TES could not defeat high efficiency oil boilers in terms of running costs. Therefore, the results in the present study indicates that Strategy C can help increase the retrofit rates of CAWHPs into the domestic buildings in off-gas grid areas, where the heating systems highly rely on oil boilers [18], due to their better operating costs and carbon emissions compared to these fossil-fuel boilers.

## 5. Conclusions

Different load shifting control strategies for a CAWHP coupled with TES were investigated in this study. The control strategies were designed to shift the heating electrical demands from peak to off-peak hours following the electricity rates of the Powershift tariff. Three control strategies were developed with the aims to improve the system operation efficiency to obtain minimised running costs and reduced wind power curtailment. TRNSYS simulation software was used to model and simulate the system applied the developed control algorithms. The simulation results indicated that:

- If the cascade heat pump was used for the heating system, the tank size of 1.2 $m^3$ along with the tank temperature set point of 75 °C could shift wholly the house heat demand to off-peak periods with minimised running costs.
- Strategy C in which the cascade heat pump was forced to charge the TES at 3 am (low electricity rate) and 2 pm (high ambient temperatures) and then discharge in the morning and afternoon, respectively, was the best load shifting strategy. It could obtain minimised running costs, perfect peak load shifting, high levels of thermal comfort and high proportions of wind energy integrated into the grid, compared with the other two strategies.
- If the cascade heat pump was not controlled (Base Case scenario), its running costs were highest and it negatively affected on the grid, whilst thermal comfort could be achieved well.
- Strategy C could help the cascade heat pump save operating costs (16 - 34 %) and carbon emissions (20 - 37 %) when it was retrofitted into the houses using oil boilers.
- While the cascade heat pump applied Strategy C could not beat high efficiency gas boilers (70 – 90 %) in terms of running costs, it could acquire carbon savings from 3 % to 24 %.

## Acknowledgement

The authors would like to acknowledge the support funding from the European Commission via H2020, IDEAS [Grant number: 815271]. The authors also thank for the financial contribution from the European Commission via H2020, CHESS-SETUP project [Grant number: 680556] and CHESTER project [Grant number: 764042]. Finally, the authors are grateful to the European Union for the funding through Interreg VA SPIRE 2 project [Grant number: IVA5038].

## References

[1] Energy Consumption in the UK July 2017, Tech. rep., Department for Business, Energy and Industrial Strategy, https://www.gov.uk/government/statistics/digest-of-uk-energy-statistics-dukes-2017-main-report [Accessed 04-09-2019].

[2] Provisional estimates of UK Greenhouse Gas emissions for 2015, including quarterly emissions for 4th quarter 2015, Tech. rep., Department of Energy and Climate Change, https://www.gov.uk/government/statistics/provisional-uk-greenhouse-gas-emissions-national-statistics-2015 [Accessed 04-09-2019].

[3] Emissions from Heat, Tech. rep., Department of Energy and Climate Change, https://www.gov.uk/government/statistics/uk-emissions-from-heat [Accessed 04-09-2019].

[4] Climate change act 2008, Tech. rep., Parliament of the United Kingdom, http://www.legislation.gov.uk/ukpga/2008/27/pdfs/ukpga_20080027_en.pdf [Accessed 11-10-2018].

[5] N. Kelly, J. Cockroft, Analysis of retrofit air source heat pump performance: Results from detailed simulations and comparison to field trial data, Energy and Buildings 43 (1) (2011) 239–245. doi:10.1016/j.enbuild.2010.09.018.

[6] L. Cabrol, P. Rowley, Towards low carbon homes - a simulation analysis of building-integrated air-source heat pump systems, Energy and Buildings 48 (2012) 127–136. doi:10.1016/j.enbuild.2012.01.019.

[7] Detailed analysis from the first phase of the Energy Saving Trust's heat pump field trial 2012, Tech. rep., Department of Energy and Climate Change, https://www.gov.uk/government/publications/greenhouse-gas-reporting-conversion-factors-2018 [Accessed 5-10-2018].

[8] BS EN 442-2: Radiators and Convectors Part 2: Test Methods and Rating, Tech. rep., BSI.

[9] H. W. Jung, H. Kang, W. J. Yoon, Y. Kim, Performance comparison between a single-stage and a cascade multi-functional heat pump for both air heating and hot water supply, International Journal of Refrigeration 36 (5) (2013) 1431 – 1441. doi:https://doi.org/10.1016/j.ijrefrig.2013.03.003.

[10] J. Wu, Z. Yang, Q. Wu, Y. Zhu, Transient behavior and dynamic performance of cascade heat pump water heater with thermal storage system, Applied Energy 91 (1) (2012) 187 – 196. doi:https://doi.org/10.1016/j.apenergy.2011.09.020.

[11] K. X. Le, M. J. Huang, N. N. Shah, C. Wilson, P. M. Artain, R. Byrne, N. J. Hewitt, Techno-economic assessment of cascade air-to-water heat pump retrofitted into residential buildings using experimentally validated simulations, Applied Energy 250 (2019) 633 – 652. doi:https://doi.org/10.1016/j.apenergy.2019.05.041.

[12] N. J. Kelly, P. G. Tuohy, A. D. Hawkes, Performance assessment of tariff-based air source heat pump load shifting in a uk detached dwelling featuring phase change-enhanced buffering, Applied Thermal Engineering 71 (2) (2014) 809 – 820, special Issue: MICROGEN III: Promoting the transition to high efficiency distributed energy systems. doi:https://doi.org/10.1016/j.applthermaleng.2013.12.019.

[13] P. J. Luickx, L. M. Helsen, W. D. D'haeseleer, Influence of massive heat-pump introduction on the electricity-generation mix and the ghg effect: Comparison between belgium, france, germany and the netherlands, Renewable and Sustainable Energy Reviews 12 (8) (2008) 2140 – 2158. doi:https://doi.org/10.1016/j.rser.2007.01.030.

[14] Annual renewable energy constraint and curtailment - Report 2017, http://www.eirgridgroup.com/Annual-Renewable-Constraint-and-Curtailment-Report-2017-V1.pdf [Accessed 01-07-2019] (2018).

[15] K. Chua, S. Chou, W. Yang, Advances in heat pump systems: A review, Applied Energy 87 (12) (2010) 3611 – 3624. doi:https://doi.org/10.1016/j.apenergy.2010.06.014.

[16] L. Zhang, Y. Jiang, J. Dong, Y. Yao, Advances in vapor compression air source heat pump system in cold regions: A review, Renewable and Sustainable Energy Reviews 81 (2018) 353 – 365. doi:https://doi.org/10.1016/j.rser.2017.08.009.

[17] Z. Ma, Z. Yang, Y. Yao, Y. Yu, Analysis of using air-source heat pump water chiller-heater units in the cold regions, Nuantong Kongtiao/HVAC 31 (3) (2001) 28.

[18] Evidence Gathering – Low Carbon Heating Technologies, Tech. rep., Department for Business, Energy and Industrial Strategy, https://assets.publishing.service.gov.uk/government/uploads/system/uploads/attachment_data/file/565248/Heat_Pumps_Combined_Summary_report_-_FINAL.pdf [Accessed 5-10-2018].

[19] N. J. Hewitt, Heat pumps and energy storage – the challenges of implementation, Applied Energy 89 (1) (2012) 37 – 44. doi:10.1016/j.apenergy.2010.12.028.

[20] D. Fischer, H. Madani, On heat pumps in smart grids: A review, Renewable and Sustainable Energy Reviews 70 (2017) 342 – 357. doi:https://doi.org/10.1016/j.rser.2016.11.182.

[21] T. Q. Péan, J. Salom, R. Costa-Castelló, Review of control strategies for improving the energy flexibility provided by heat pump systems in buildings, Journal of Process Control 74 (2019) 35 – 49, efficient energy management. doi:https://doi.org/10.1016/j.jprocont.2018.03.006.

[22] A. Arteconi, N. Hewitt, F. Polonara, Domestic demand-side management (dsm): Role of heat pumps and thermal energy storage (tes) systems, Applied Thermal Engineering 51 (1) (2013) 155 – 165. doi:https://doi.org/10.1016/j.applthermaleng.2012.09.023.

[23] J. Guo, J. Wu, R. Wang, S. Li, Experimental research and operation optimization of an air-source heat pump water heater, Applied Energy 88 (11) (2011) 4128 – 4138. doi:https://doi.org/10.1016/j.apenergy.2011.04.012.

[24] O. Ibrahim, F. Fardoun, R. Younes, H. Louahlia-Gualous, Air source heat pump water heater: Dynamic modeling, optimal energy management and mini-tubes condensers, Energy 64 (2014) 1102 – 1116. doi:https://doi.org/10.1016/j.energy.2013.11.017.

[25] R. D. Coninck, R. Baetens, B. Verbruggen, J. Driesen, D. Saelens, L. Helsen, Modelling and simulation of a grid connected photovoltaic heat pump system with thermal energy storage using modelica, in:

8th International Conference on System Simulation in Buildings (SSB2010), 2010.

[26] TRNSYS 17, a TRaNsient SYstem Simulation program – vol. 3- Component Library Overview, http://www.trnsys.com/assets/docs/03-ComponentLibraryOverview.pdf [Accessed 5-10-2018].

[27] N. N. Shah, C. Wilson, M. J. Huang, N. J. Hewitt, Analysis on field trial of high temperature heat pump integrated with thermal energy storage in domestic retrofit installation, Applied Thermal Engineering 143 (2018) 650 – 659. doi:https://doi.org/10.1016/j.applthermaleng.2018.07.135.

[28] Daikin Altherma HT 11, Daikin UK Limited, http://www.daikin.co.uk/domestic/needs/heating/air-water-heatpumps-ht/index.jsp [Accessed 04-09-2019].

[29] SketchUp, https://www.sketchup.com/[Accessed 10-06-2018].

[30] O. QUEVILLON, L. Lamarche, S. Kajl, Couplage d'un Échangeur air-sol pour augmenter la performance en chauffage d'une pompe À chaleur À air, in: XIIIème Colloque Interuniversitaire Franco-Québécois sur la Thermique des Systèmes 22-24 mai 2017, LUSAC Saint-Lô, France, 2017.

[31] Soni (System Operator for Northern Ireland), http://www.soni.ltd.uk/ [Accessed 01-07-2019] (2019).

[32] Northern Ireland electricity tariffs, https://touch.nihe.gov.uk/latest_tariffs [Accessed 01-07-2019] (2018).

[33] EIRGRID, http://smartgriddashboard.eirgrid.com/#all/co2[Accessed 30-06-2019].

[34] K. X. Le, N. Shah, M. J. Huang, N. J. Hewitt, High temperature air-water heat pump and energy storage: Validation of trnsys models, in: Proceedings of the World Congress on Engineering and Computer Science 2017 Vol II, October 25-27, 2017, San Francisco, USA, 2017.

[35] The Northern Ireland House Condition Survey 2017, https://www.nihe.gov.uk/My-Housing-Executive [Accessed 04-09-2019].

[36] Home Heating Oil, http://www.consumercouncil.org.uk/consumers/save-money/energy/home-heating-oil [Accessed 08-10-2018].

[37] Gas price comparison for Greater Belfast and Larne area 2018, http://www.consumercouncil.org.uk/search?search_api_fulltext=filestore+documents+Gas+Price+Comparison+Table+April+2018+pdf [Accessed 08-10-2018].

[38] Greenhouse gas reporting: conversion factors 2017 - GOV.UK, Tech. rep., Department for Business, Energy and Industrial Strategy, https://www.gov.uk/government/publications/greenhouse-gas-reporting-conversion-factors-2017 [Accessed 03-02-2018].